JMR Journal of Meteorological Research

# Comparison of Sunshine Duration Measurements between a Jordan Sunshine Recorder and Three Automatic Sensors at Shangdianzi GAW Station

Huaigang ZHOU, Weijun QUAN, Zhenfa WANG, Xiaolan LI, Yingruo LI, Hujia ZHAO

**Citation:** Zhou, H. G., W. J. Quan, Z. F. Wang, et al., 2021: Comparison of sunshine duration measurements between a Jordan sunshine recorder and three automatic sensors at Shangdianzi GAW station. *J. Meteor. Res.*, **35**(4), 716–728, doi: 10.1007/s13351–021–0158–3

View online: http://jmr.cmsjournal.net/article/doi/10.1007/s13351–021–0158–3

## Related articles that may interest you

Shortened Duration of Global Warming Slowdowns with Elevated Greenhouse Gas Emissions

Journal of Meteorological Research. 2021, 35(2), 225 https://doi.org/10.1007/s13351–021–0134–y

Reconstructing Missing Hourly Real–Time Precipitation Data Using a Novel Intermittent Sliding Window Period Technique for Automatic Weather Station Data

Journal of Meteorological Research. 2017, 31(4), 774 https://doi.org/10.1007/s13351–017–6084–8

Evaluation of the Relationship between Blocking Patterns and Duration of Spring Frost Waves: The Case of Iran

Journal of Meteorological Research. 2020, 34(3), 586 https://doi.org/10.1007/s13351–020–9140–8

Validation of Column–Averaged Dry–Air Mole Fraction of $CO_2$ Retrieved from OCO–2 Using Ground–Based FTS Measurements

Journal of Meteorological Research. 2018, 32(3), 433 https://doi.org/10.1007/s13351–018–7118–6

High Spatial Resolution and High Temporal Frequency (30–m/15–day) Fractional Vegetation Cover Estimation over China Using Multiple Remote Sensing Datasets: Method Development and Validation

Journal of Meteorological Research. 2021, 35(1), 128 https://doi.org/10.1007/s13351–021–0017–2

Perturbations in Earth's Atmosphere over An Indian Region during the Total Solar Eclipse on 22 July 2009

Journal of Meteorological Research. 2019, 33(4), 784 https://doi.org/10.1007/s13351–019–8056–7

# Comparison of Sunshine Duration Measurements between a Jordan Sunshine Recorder and Three Automatic Sensors at Shangdianzi GAW Station

Huaigang ZHOU[1,2], Weijun QUAN[1,2*], Zhenfa WANG[1,2], Xiaolan LI[3], Yingruo LI[1,2], and Hujia ZHAO[3]

1 *Institute of Urban Meteorology*, *China Meteorological Administration*, *Beijing* 100089
2 *Environmental Meteorology Forecast Center of Beijing–Tianjin–Hebei*, *Beijing* 100089
3 *Institute of Atmospheric Environment*, *China Meteorological Administration*, *Shenyang* 110016

(Received September 12, 2020; in final form April 15, 2021)

ABSTRACT

We used parallel sunshine duration datasets obtained with a Jordan sunshine recorder and three automatic sunshine duration sensors to investigate the differences between these instruments. We used measurements obtained at Shangdianzi (SDZ) regional Global Atmosphere Watch (GAW) station with a Jordan sunshine recorder, a DFC2 photoelectric sunshine meter, a CHP1 pyrheliometer, and two CMP11 pyranometers from 1 January to 5 July 2019 and from 3 November 2020 to 28 February 2021. The results showed that the daily sunshine duration measurements obtained from the Jordan sunshine recorder were comparable with those from the DFC2 meter and the CMP11 pyranometers under all-sky conditions, but were considerably different from those observed by the CHP1 pyrheliometer. An analysis of potential influencing factors showed that the solar zenith angle, the spectral range of the automatic sensors, the relative humidity, and the sky conditions were the main factors affecting the measurements of sunshine duration between the Jordan sunshine recorder and three automatic sensors. We proposed a simple linear regression function—the DFC2-equivalent sunshine duration estimation (DFCESD) model—to guarantee the consistency of the long-term sunshine duration series observed by the Jordan sunshine recorder at SDZ and the measurements from the DFC2 meter. Validation of the DFCESD model showed that the mean absolute difference (MAD) between the daily sunshine duration observed by the Jordan sunshine recorder and those from the DFC2 meter improved from −0.7 to −0.2 h day$^{-1}$, the relative deviation (RD) improved from −9.3% to −2.3%, and the root-mean-square deviation (RMSD) decreased from 1.0 to 0.8 h day$^{-1}$.

**Key words:** sunshine duration, Jordan sunshine recorder, pyrheliometer, pyranometer, Shangdianzi station

**Citation:** Zhou, H. G., W. J. Quan, Z. F. Wang, et al., 2021: Comparison of sunshine duration measurements between a Jordan sunshine recorder and three automatic sensors at Shangdianzi GAW station. *J. Meteor. Res.*, **35**(4), 716–728, doi: 10.1007/s13351-021-0158-3.

## 1. Introduction

Sunshine duration is an essential meteorological variable and represents the total time for which the sun is shining. It is a key factor in most climate processes—for example, the earth's radiative balance and the hydrological cycle (Ranzi and Rosso, 1995; Pandey et al., 2016). It is also used in sectors such as tourism, public health, agriculture, vegetation growth, and solar energy production (Sanchez-Romero et al., 2015; Wang et al., 2015; Babikir et al., 2018). Sunshine duration is affected by the atmospheric conditions and can serve as a proxy for atmospheric turbidity (Sanchez-Romero et al., 2014).

Sunshine duration has been routinely measured for > 160 yr since J. F. Campbell designed the first sunshine recorder in 1853. This was improved by G. G. Stokes in 1880 and later renamed the Campbell–Stokes sunshine recorder (CSSR). The CSSR uses a glass globe to focus incoming solar radiation and burn a track onto a card placed within its focal range. The sunshine duration record is retrieved from the track burned onto the recording card (Stanhill, 2003; Sanchez-Lorenzo et al., 2013). The CSSR can measure sunshine duration at low elevation angles and therefore has been widely used in many

Supported by the National Key Research and Development Program of China (2017YFB0504002) and Special Fund for Basic Scientific Research of Institute of Urban Meteorology (2017).

*Corresponding author: quanquan78430@163.com

© The Chinese Meteorological Society and Springer-Verlag Berlin Heidelberg 2021

parts of the world, especially in high-latitude regions, for > 100 yr (Horseman et al., 2008). In 1962, the CSSR was adopted by the World Meteorological Organization (WMO) as the Interim Reference Sunshine Recorder through which sunshine data published worldwide were adjusted (Matuszko, 2015).

In parallel with the development of the CSSR, during the mid-1880s, James B. Jordan and Frederic Gaster improved an instrument developed by Jordan's father in the 1830s. They introduced a new photographic sunshine recorder (the Jordan sunshine recorder) in 1885, and subsequently, a new version of the device in 1888 (Jordan, 1888; Sanchez-Romero et al., 2014). The Jordan sunshine recorder has a simple construction and the working part consists of a dark cylindrical chamber mounted on a suitable stand, which can be adjusted to suit the latitude of the station. This cylinder is pierced by two small rectangular apertures and the rays of sunlight pass directly through these apertures and are received onto the sensitized surface of a photographic paper placed inside. The Jordan sunshine recorder has been widely used to record sunshine duration at meteorological stations around the world and has produced a large number of long-term records.

In recent decades, much progress has been made to develop automatic sensors for measuring sunshine duration. For instance, thermoelectric sensors, such as the pyrheliometer and pyranometer, use a thermopile as a detector to measure solar irradiance directly (WMO, 2006; Hinssen and Knap, 2007) and then convert this into sunshine duration based on a threshold. Photoelectric sunshine meters use a photodiode to obtain solar irradiance (Wood et al., 2003; Matuszko, 2015; Yang et al., 2017).

The threshold is a key parameter in measuring sunshine duration and is generally assumed to be constant (Gueymard, 1993). Jaenicke and Kasten (1978) pointed out that a large variety of thresholds are suited to different CSSRs. Helmes and Jaenicke (1984) described the influence of different types of recording cards on sunshine duration measurements made by the CSSR. Brázdil et al. (1994) stressed the importance of using the same type of card to compare different sunshine duration series. The threshold value is usually different for individual sunshine duration instrument and varies with the observing season, the site, and the weather conditions (Painter, 1981; Zhang and Tan, 2000; Kerr and Tabony, 2004; Legg, 2014; Matuszko, 2015; Baumgartner et al., 2018).

In the eighth session of the Commission for Instruments and Methods of Observation held in 1981, the WMO recommended use of the direct normal solar irradiance (> 120 W $m^{-2}$) as a threshold for the determination of sunshine duration to solve this consistency issue (Painter, 1981; WMO, 1982; Li et al., 1989; Baumgartner et al., 2018). The sunshine duration values obtained from the CSSR, the Jordan sunshine recorder, and automatic sunshine sensors are considerably different as a result of the different principles and technology adopted by these instruments (Zhang and Tan, 2000; Kerr and Tabony, 2004; Legg, 2014; Matuszko, 2015; Baumgartner et al., 2018).

The Jordan sunshine recorder has a long history of sunshine duration measurements at most of the meteorological observation stations in China. A photoelectric sensor, the DFC2 photoelectric sunshine meter, was recently recommended by the China Meteorological Administration (CMA) as an alternative to improve automatic sunshine duration measurements. It is therefore important to determine the consistency of sunshine duration measurement series when the Jordan sunshine recorder is replaced by the DFC2 meter. Previous investigations have mainly focused on comparing the sunshine duration measurements obtained from the Jordan sunshine recorder and automatic sensors under various sky conditions, rather than elucidating the mechanisms that affect the difference in sunshine duration between these instruments.

Section 2 describes the sunshine duration instruments operated at Shangdianzi regional atmospheric background station (SDZ). These instruments consist of the Jordan sunshine recorder, the DFC2 meter, a CHP1 pyrheliometer, and two CMP11 pyranometers. Section 3 compares the daily sunshine duration measurements obtained from these instruments under various sky conditions and discusses the mechanisms and major factors affecting the sunshine duration measurements using hourly sunshine duration data. To guarantee the consistency of the sunshine duration data, Section 4 establishes a linear regression model to convert the daily sunshine duration measurements from the Jordan sunshine recorder to those of the DFC2. Section 5 presents our discussion and conclusions.

## 2. Data and methods

### 2.1 *Site and instruments*

The SDZ (40.65°N, 117.12°E; 293.3 m a.s.l.) was founded by the CMA in 1981 and became one of the earliest regional Global Atmosphere Watch (GAW) stations of the WMO in China. It is located in the northern North China Plain and provides representative background data because there are only a few small villages with a sparse population around this site; anthropogenic

emission sources are therefore insignificant (Lin et al., 2008).

We performed two parallel experiments at SDZ over the time periods 1 January–5 July 2019 and 3 November 2020–28 February 2021. A total of 3601 hourly and 301 daily sunshine duration measurements were produced from both the Jordan sunshine recorder and three automatic sensors.

A Jordan sunshine recorder (Tianjin Meteorological Instrument Factory) has been used to record sunshine duration at the Shangdianzi meteorological observation station (the predecessor of the SDZ) since 1958. It is located at the top of a 1.5-m high steel column in the meteorological observation field of the SDZ (denoted as ① in Fig. 1a). It is a manually operated sunshine duration recorder and the recording paper has to be chemically treated and replaced by an operator every day during the observation period (Sanchez-Romero et al., 2015).

The DFC2 photoelectric sunshine meter (Huayun Sounding Meteorological Technology) has been used to observe sunshine duration at the SDZ since 1 January 2019. It is mounted at the top of another steel column, ~1.0 m north of the column with the Jordan sunshine recorder (denoted as ② in Fig. 1a). The DFC2 meter consists of three parts: an HYSD-1 photoelectric sensor, a power supply system, and a mounting bracket. The HYSD-1 sensor is composed of three silicon photodiodes enveloped in a JGS3 quartz glass cylinder, through which solar radiation in the spectral range of 270–3200 nm passes without attenuation. One photodiode is exposed to all the sky to measure the total solar irradiance, whereas the other two are used to measure diffuse irradiance from the sky. The spectral range of the HYSD-1 is 400–1100 nm (Huayun Sounding, 2018).

The CHP1 pyrheliometer is mounted on a solar tracker installed on a platform at the top of the SDZ building (denoted as ③ in Fig. 1d). One CMP11 pyranometer is set to receive the total solar irradiance and the other, shaded with a shadow ball, is set to observe the diffuse irradiance (denoted as ④ in Fig. 1d). Both the CHP1 pyrheliometer and the two CMP11 pyranometers are part of the Baseline Surface Radiation System (BSRS), which has been operating at the SDZ since 1 January 2013. The BSRS is designed to measure irradiance from the sun, at-

**Fig. 1.** Instruments used to measure sunshine duration at the Shangdianzi regional atmospheric background station (SDZ). (a) The Jordan sunshine recorder ① and the DFC2 photoelectric meter ②. (b) The Jordan sunshine recorder and its cylindrical chamber. (c) The HYSD-1 photoelectric sensor, one of the key components of the DFC2 meter. (d) The CHP1 pyrheliometer ③ and the CMP11 pyranometers ④.

mosphere, and land surface based on the criteria provided by the Baseline Surface Radiation Network. The BSRS has a sampling frequency of 1 Hz and data storage interval of 1 min (Ohmura et al., 1998). Both the CHP1 and CMP11 instruments are manufactured by Kipp & Zonen.

The CHP1 is a high-precision pyrheliometer designed to measure direct solar irradiance from the solar disk within a solid angle of 5°. It uses a thermopile as a detector to measure the amount of solar radiation reaching the earth's surface in the range of 280–4000 nm (Kipp & Zonen, 2008). The CMP11 pyranometer is fully compliant with the ISO-9060 secondary standard pyranometer performance category [the highest International Organization for Standardization (ISO) performance criteria for a pyranometer] and is recommended by the WMO for measurements of the total solar irradiance or diffuse irradiance. It has some new features and benefits, such as a low dome thermal offset error (the zero-offset due to changes in temperature is less than ±2 W $m^{-2}$ at 5-K $h^{-1}$ temperature change), an excellent cosine/directional response (directional error less than ±10 W $m^{-2}$), an excellent long-term stability of the sensitivity, and an excellent linearity performance (nonlinearity less than ±0.6%). It works in the spectral range of 305–2800 nm (Kipp & Zonen, 2016). The two CMP11 pyranometers are ventilated to improve the reliability and accuracy of the measurements and to reduce maintenance, such as the alleviation of the thermal offset and auto-cleaning the dirt from snow, frost, precipitation, dust, and airborne pollutants. All radiometers of the BSRS at the SDZ are calibrated every one or two years by the National Center for Meteorological Metrology to guarantee that their measurements are trackable to the radiation measurement criteria of the WMO.

### 2.2 *Data for sunshine duration*

We used hourly sunshine duration data from the Jordan sunshine recorder, the DFC2 meter, the CHP1 pyrheliometer, and the CMP11 pyranometers and processed the data as follows.

(1) The hourly sunshine duration data obtained by the Jordan sunshine recorder ($U_{JR}$) were extracted from the Monthly Report of Surface Meteorological Observations.

(2) The 1-min resolution raw data of the DFC2 meter were used to calculate the hourly sunshine duration data ($U_{DFC2}$).

(3) The 1-min direct normal solar irradiance observed by the CHP1 pyrheliometer was recorded in the raw data file of the BSRS at the SDZ. At first, the method presented by Long and Shi (2008) was used to carry out quality control tests on the raw data. The normal solar irradiance data that passed the quality control test were then used, along with the threshold (120 W $m^{-2}$), to determine the hourly sunshine duration ($U_{CHP1}$).

(4) The acquisition of the hourly sunshine duration from the CMP11 pyranometers ($U_{CMP11}$) was relatively complex. At first, the direct solar irradiance on a horizontal surface ($E_h$) was calculated by subtracting the diffuse irradiance observed by one CMP11 pyranometer ($E_d$) from total solar irradiance observed by the other CMP11 pyranometer ($E_g$) [Eq. (1)]. The direct normal solar irradiance ($E_n$) was then derived according to $E_h$ and the cosine of the solar zenith angle ($\theta_z$) by using Eqs. (2)–(3). The number of $E_n$ values > 120 W $m^{-2}$ in an hour was then used as the hourly value of $U_{CMP11}$.

The equations used to derive $U_{CMP11}$ are:

$$E_h = E_g - E_d, \tag{1}$$

$$E_n = E_h/\mu, \tag{2}$$

$$\mu = \cos(\theta_z), \tag{3}$$

where $\mu$ is the cosine of $\theta_z$, which can be calculated from the latitude and longitude of the observation station and the observing time (Iqbal, 1983).

### 2.3 *Meteorological data*

We applied a meteorological dataset to determine whether meteorological factors affected the observations of sunshine duration from different instruments. The dataset consisted of hourly data for the temperature ($t$; °C), relative humidity ($f$), visibility ($S_m$; km), and wind speed ($v$; m $s^{-1}$) observed by an automatic weather station at the SDZ.

Because manual observations of the cloud cover at the SDZ were canceled in 2014, a cloud dataset from Miyun station (40.38°N, 116.87°E; 71.8 m a.s.l.), about 30 km from the SDZ, was used. This dataset consists of the cloud cover recorded by the operator at 0800, 1100, 1400, and 1700 Beijing Time (BT). Unfortunately, manual observations of the cloud cover at Miyun station were also canceled in April 2020. We therefore used 184 daily observations of cloud cover over the time period 1 January–5 July 2019 at Miyun station to evaluate the performance of the Jordan sunshine recorder and three automatic sensors under various sky conditions.

### 2.4 *Assessment methods*

We selected a series of statistical parameters—the mean absolute difference (MAD), the relative deviation (RD), the root-mean-square deviation (RMSD), and the correlation coefficient ($r$)—to illustrate the differences among the sunshine duration measurements obtained from different instruments. The definitions of these

mathematical parameters are:

$$\mathrm{MAD} = \frac{1}{n}\sum_{i=1}^{n}(U_{B,i} - U_{A,i}), \tag{4}$$

$$\mathrm{RD} = \frac{1}{n}\sum_{i=1}^{n}\frac{U_{B,i} - U_{A,i}}{U_{A,i}} \times 100\%, \tag{5}$$

$$\mathrm{RMSD} = \sqrt{\frac{1}{n}\sum_{i=1}^{n}(U_{B,i} - U_{A,i})^2}, \tag{6}$$

$$r = \frac{\sum_{i=1}^{n}(U_{B,i} - \overline{U}_B)(U_{A,i} - \overline{U}_A)}{\sqrt{\sum_{i=1}^{n}(U_{B,i} - \overline{U}_B)^2}\sqrt{\sum_{i=1}^{n}(U_{A,i} - \overline{U}_A)^2}}, \tag{7}$$

where $U_{A,i}$ and $U_{B,i}$ represent the $i$th measurements of sunshine duration from instruments $A$ and $B$, respectively, $\overline{U}_A$ and $\overline{U}_B$ are the mean values of $U_{A,i}$ and $U_{B,i}$, and $n$ is the number of samples.

## 3. Comparison of sunshine duration measurements between the Jordan sunshine recorder and three automatic sensors

### 3.1 *Comparison of the performance under different sky conditions*

Previous studies have indicated that sunshine duration values observed on the ground are strongly affected by weather conditions (e.g., the cloud cover, cloud type, fog, and atmospheric turbidity) as well as the local topography (Matuszko, 2012; Zhu et al., 2015). However, it is not clear whether these factors have the same influence on sunshine duration measurements from the Jordan sunshine recorder and the automatic sensors.

To solve this issue, we classified all the data samples collected over the time period 1 January–5 July 2019 into three categories based on the criteria of WMO (2006) and the cloud fraction ($F_c$) records from Miyun station: cloudless sky ($F_c = 0$), partly cloudy sky ($0 < F_c < 1$), and overcast sky ($F_c = 1$). In addition, 227 daily sunshine duration measurements observed over the time periods 1 January–5 July 2019 and 3 November–15 December 2020 were taken into account in the all-sky ($0 \leqslant F_c \leqslant 1$) category. Table 1 lists the statistical parameters of the comparisons between the daily sunshine duration derived from the Jordan sunshine recorder and three automatic sensors under various sky conditions.

In general, the less cloud in the sky, the more daily sunshine duration is observed on the ground. For example, the values for the mean daily sunshine duration derived from the DFC2 meter ($\overline{U}_{\mathrm{DFC2}}$) were 11.0 and 7.8 h day$^{-1}$ when the sky was cloudless and partly cloudy, respectively, whereas it was only 3.2 h day$^{-1}$ when the sky was overcast. Analogous trends were also found in the daily sunshine duration from the CHP1 pyrheliometer ($\overline{U}_{\mathrm{CHP1}}$), the CMP11 pyranometers ($\overline{U}_{\mathrm{CMP11}}$), and the Jordan sunshine recorder ($\overline{U}_{\mathrm{JR}}$).

Figure 2a shows that $U_{\mathrm{DFC2}}$ and $U_{\mathrm{JR}}$ are generally comparable, with MAD of −0.1 h day$^{-1}$, RD of −1.5%, RMSD of 1.2 h day$^{-1}$, and $r$ of 0.944. Figure 2b shows that the MAD between $U_{\mathrm{DFC2}}$ and $U_{\mathrm{JR}}$ under a cloudless sky is 0.4 h day$^{-1}$ (RD = 4.2%). The variable $U_{\mathrm{JR}}$ is generally less than $U_{\mathrm{DFC2}}$ when the sky is clear. Because the actual value of solar irradiance that causes a "burn" point on the recording paper of the Jordan sunshine recorder is usually greater than the threshold of 120 W m$^{-2}$, the Jordan sunshine recorder measurement is often less than its nominal value under a cloudless sky (Zhang and Tan, 2000). By contrast, the MADs between $U_{\mathrm{DFC2}}$ and $U_{\mathrm{JR}}$ are −0.3 and −1.5 h day$^{-1}$ under partly cloudy and overcast conditions, respectively. This is mostly caused by the influence of clouds—that is, in the presence of high or convective clouds, short high-intensity bursts of sunlight create an overlapping tracing effect on the recording card of the Jordan sunshine recorder, which overestimates the sunshine duration (Hoyt, 1977; Raju and Kumar, 1982; Hinssen and Knap, 2007; Matuszko, 2012).

We adopted a classification scheme for characterizing the agreement/disagreement among individual sunshine duration records (Urban and Zając, 2017) to show the distribution of the differences in sunshine duration between the DFC2 meter and Jordan sunshine recorder. Four grades were classified in terms of the difference in daily sunshine duration between the DFC2 meter and the Jordan sunshine recorder ($U_{\mathrm{DFC2}} - U_{\mathrm{JR}}$): (1) an insignificant grade (C1), within the margin of error [−0.1 h, 0.1 h]; (2) small grades, which consist of a small negative grade level (−C2) [−0.5 h, −0.1 h) and a small positive grade level (C2) (0.1 h, 0.5 h] within the margin of error; (3) medium grades, composed of a medium negative region (−C3) within the margin of error [−1.5 h, −0.5 h) and a medium positive region (C3) within the margin of error (0.5 h, 1.5 h]; and (4) high grades, which consist of a high negative region (−C4) with a margin of error < −1.5 h and a high positive region (C4) with a margin of error > 1.5 h.

Figure 2e shows that about 83.5% of ($U_{\mathrm{DFC2}} - U_{\mathrm{JR}}$) under cloudless skies fall within positive grades (45.9% for C3 and 37.6% for C2). The percentages falling within the negative (−C2) and insignificant (C1) grades are 5.4% and 10.8%, respectively. In the presence of partly

**Table 1.** Statistical parameters of daily sunshine duration derived from the Jordan sunshine recorder, the DFC2 meter, the CHP1 pyrheliometer, and the CMP11 pyranometers

| Automatic instrument | Manual instrument | Sky condition | $\overline{U}_{auto}$ (h day$^{-1}$) | $\overline{U}_{JR}$ (h day$^{-1}$) | MAD (h day$^{-1}$) | RD (%) | RMSD (h day$^{-1}$) | $r$ | $n$ |
|---|---|---|---|---|---|---|---|---|---|
| DFC2 | Jordan sunshine recorder | All-sky | 7.7 | 7.8 | −0.1 | −1.5 | 1.2 | 0.944 | 227 |
| | | Cloudless | 11.0 | 10.6 | 0.4 | 4.2 | 0.5 | 0.988 | 37 |
| | | Partly cloudy | 7.8 | 8.1 | −0.3 | −3.2 | 1.0 | 0.955 | 121 |
| | | Overcast | 3.2 | 4.7 | −1.5 | −31.1 | 2.3 | 0.912 | 26 |
| CHP1 | Jordan sunshine recorder | All-sky | 8.0 | 7.8 | 0.2 | 2.7 | 3.4 | 0.551 | 227 |
| | | Cloudless | 8.5* | 10.6* | −2.1 | −20.0 | 4.4 | 0.328 | 37 |
| | | Partly cloudy | 8.5 | 8.1 | 0.4 | 4.5 | 3.2 | 0.575 | 121 |
| | | Overcast | 6.7 | 4.7 | 2.0 | 43.0 | 3.6 | 0.757 | 26 |
| CMP11 | Jordan sunshine recorder | All-sky | 7.9 | 7.8 | 0.1 | 0.7 | 1.1 | 0.952 | 227 |
| | | Cloudless | 11.1 | 10.6 | 0.5 | 5.0 | 0.6 | 0.986 | 37 |
| | | Partly cloudy | 8.0 | 8.1 | −0.1 | −0.8 | 1.0 | 0.960 | 121 |
| | | Overcast | 3.5 | 4.7 | −1.2 | −25.7 | 2.0 | 0.946 | 26 |

Note: MAD: mean absolute difference of the daily sunshine duration (h day$^{-1}$); RD: relative deviation; RMSD: root-mean-square deviation (h day$^{-1}$); $r$: correlation coefficient; $n$: number of samples. The variables $\overline{U}_{auto}$ and $\overline{U}_{JR}$ represent the mean values of daily sunshine duration (h day$^{-1}$) observed by the automatic instruments and the Jordan sunshine recorder, respectively. *At a significance level of 0.05, the $U$-test results show that the mean values of the daily sunshine duration observed by the automatic sensors and the Jordan sunshine recorder are significantly different.

cloudy skies, the values are distributed evenly across all grades, except C4 (0.8%), with frequencies of 22.3% (C3, C1), 20.7% (−C3), 11.6% (C2, −C2), and 10.7% (−C4). Under overcast conditions, 61.6% of the values fall within the negative regions, with 38.5% for −C4 and 15.4% for −C3. For all-sky conditions, a relatively balanced distribution of the frequency occurs over all grades: C3, 28.2%; C1, 18.9%; C2, 17.2%; −C3, 13.2%; −C4, 10.6%; −C2, 9.3%; and C4, 2.6%.

The variable $U_{CHP1}$ is considerably different from $U_{JR}$ under various sky conditions (Fig. 3). For example, although the MAD between $U_{CHP1}$ and $U_{JR}$ under all-sky conditions is 0.2 h day$^{-1}$ (RD = 2.7%), the RMSD is very high (3.4 h day$^{-1}$) and $r$ is only 0.551. In particular, $U_{CHP1}$ is clearly lower than $U_{JR}$ under cloudless skies, which may result from the incorrect tracking of the solar position by the CHP1 pyrheliometer. The MAD between $U_{CHP1}$ and $U_{JR}$ under partly cloudy and overcast conditions is 0.4 h day$^{-1}$ (RD = 4.5%) and 2.0 h day$^{-1}$ (RD = 43.0%), respectively (Figs. 3c, d). In these cases, the total percentages of ($U_{CHP1} - U_{JR}$) falling in grades C3 and C4 are 65.3% and 73.1% for partly cloudy and overcast sky conditions, respectively. Note that the CHP1 pyrheliometer has a full opening angle of 5°, which allows part of the solar irradiance reflected by the cloud to enter the radiometer housing, leading to higher sunshine duration measurements under partly cloudy or overcast skies.

Figure 4 shows the scatterplots and the frequencies of the daily values of $U_{CMP11}$ against $U_{JR}$ under all-sky, cloudless sky, partly cloudy, and overcast conditions. Figure 4a shows that the MAD is 0.1 h day$^{-1}$, the RD is 0.7%, and the RMSD is 1.1 h day$^{-1}$ for all-sky conditions, which implies that the daily sunshine duration measurements from the CMP11 pyranometers are very close to those from the Jordan sunshine recorder. The variable $U_{CMP11}$ shows a systematically lower trend relative to $U_{JR}$ when the sky is cloudy, where the MAD is −1.2 h day$^{-1}$ and the RD reaches −25.7% (Fig. 4d). Figure 4f clearly shows ~54.1% and ~32.4% of ($U_{CMP11} - U_{JR}$) in grades C3 and C2 under a cloudless sky, whereas the percentages of ($U_{CMP11} - U_{JR}$) falling within −C4, −C3, and −C2 are 38.5%, 15.4%, and 7.7%. The irradiance reaching the pyranometers may be obstructed in the presence of high or convective clouds, whereas a short period of high-intensity sunlight could create a prolonged effect on the recording card of the Jordan sunshine recorder. This means that the Jordan sunshine recorder will measure a longer duration of sunshine in contrast to the CMP11 pyranometer.

### 3.2 *Factors potentially influencing sunshine duration measurements*

To further elucidate the mechanisms affecting sunshine duration measurements, we used a high temporal (hourly) resolution dataset of sunshine duration and other meteorological elements, including solar zenith angles, to analyze the correlation between meteorological elements and differences in sunshine duration measured by the Jordan sunshine recorder and three automatic sensors. The independent variables consisted of $\mu$, $t$ (°C), $f$, $S_m$ (km), and $v$ (m s$^{-1}$). The dependent variables were the differences in sunshine duration between the measurements recorded by the Jordan sunshine recorder and the DFC2 ($\Delta U_{DFC2_JR}$), the CHP1 ($\Delta U_{CHP1_JR}$), and the CMP11 ($\Delta U_{CMP11_JR}$) sensors. It is known that dependent variables may be affected by more than one inde-

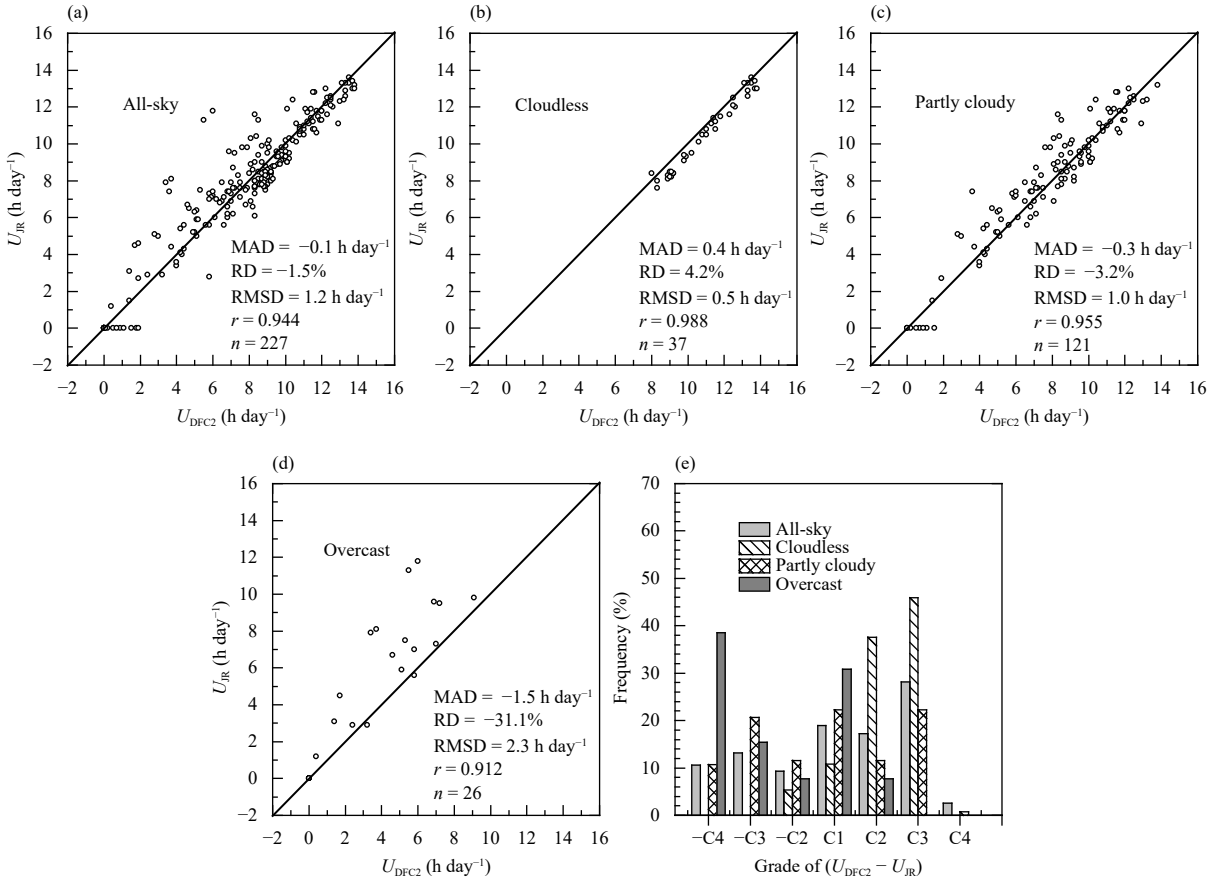


**Fig. 2.** Scatterplots of daily sunshine duration observed by the DFC2 meter ($U_{DFC2}$) versus those obtained from the Jordan sunshine recorder ($U_{JR}$) at the SDZ under (a) all-sky, (b) cloudless sky, (c) partly cloudy sky, and (d) overcast sky conditions. (e) Frequencies of differences in sunshine duration between the DFC2 meter and the Jordan sunshine recorder against the classification grades of Urban and Zając (2017).

pendent variable as a result of complex relationships. We therefore introduced the partial correlation coefficient ($r_p$) to analyze the correlation between one of the independent variables and the dependent variable without considering the other independent variables. We also adopted a multiple correlation coefficient ($r_m$) to represent the overall correlation between the dependent variable and all independent variables. Table 2 lists all the partial and multiple correlation coefficients calculated in this study.

Table 2 shows that $r_m$ between $\Delta U_{CMP11_JR}$ and all independent variables is 0.309, which is higher than the $r_m$ values of $\Delta U_{DFC2_JR}$ (0.289) and $\Delta U_{CHP1_JR}$ (0.301). All the multiple correlation coefficients pass the test at a significance level of 0.05, except $\Delta U_{CHP1_JR}$. By contrast, $r_p$ of $\mu$ has considerable negative values for $\Delta U_{DFC2_JR}$ (−0.254), $\Delta U_{CHP1_JR}$ (−0.270), and $\Delta U_{CMP11_JR}$ (−0.269), which indicate that the difference in sunshine duration decreases with increasing $\mu$ (or decreasing $\theta_z$). For the Jordan sunshine recorder, the larger value of $\theta_z$, the fewer solar rays enter the optical cylinder, which means that the sunshine duration measurement is smaller than the actual value. The two key meteorological factors influencing the difference in sunshine duration between the Jordan sunshine recorder and three automatic sensors are $t$ and $f$. This is because the air temperature and relative humidity change the photosensitivity of the recording card in the Jordan sunshine recorder (Li et al., 1989).

Figure 5 shows diurnal variation of sunshine duration, the differences in sunshine duration, the solar zenith angle, and the relative humidity calculated from the multi-day hourly dataset described in Sections 2.2 and 2.3. Figure 5a shows that the hourly sunshine duration retrieved from the Jordan sunshine recorder and three automatic sensors showed analogous patterns of diurnal variation—that is, they varied inversely with $\theta_z$. For convenience, three time periods are denoted by the dashed lines in Fig. 5. In the first period (0600–0800 BT), the sunshine duration measured by the Jordan sunshine recorder, the DFC2 sensor, and the CMP11 pyranometers increased from about zero to ~0.5 h h$^{-1}$, whereas the sunshine duration of the CHP1 pyrheliometer was relatively

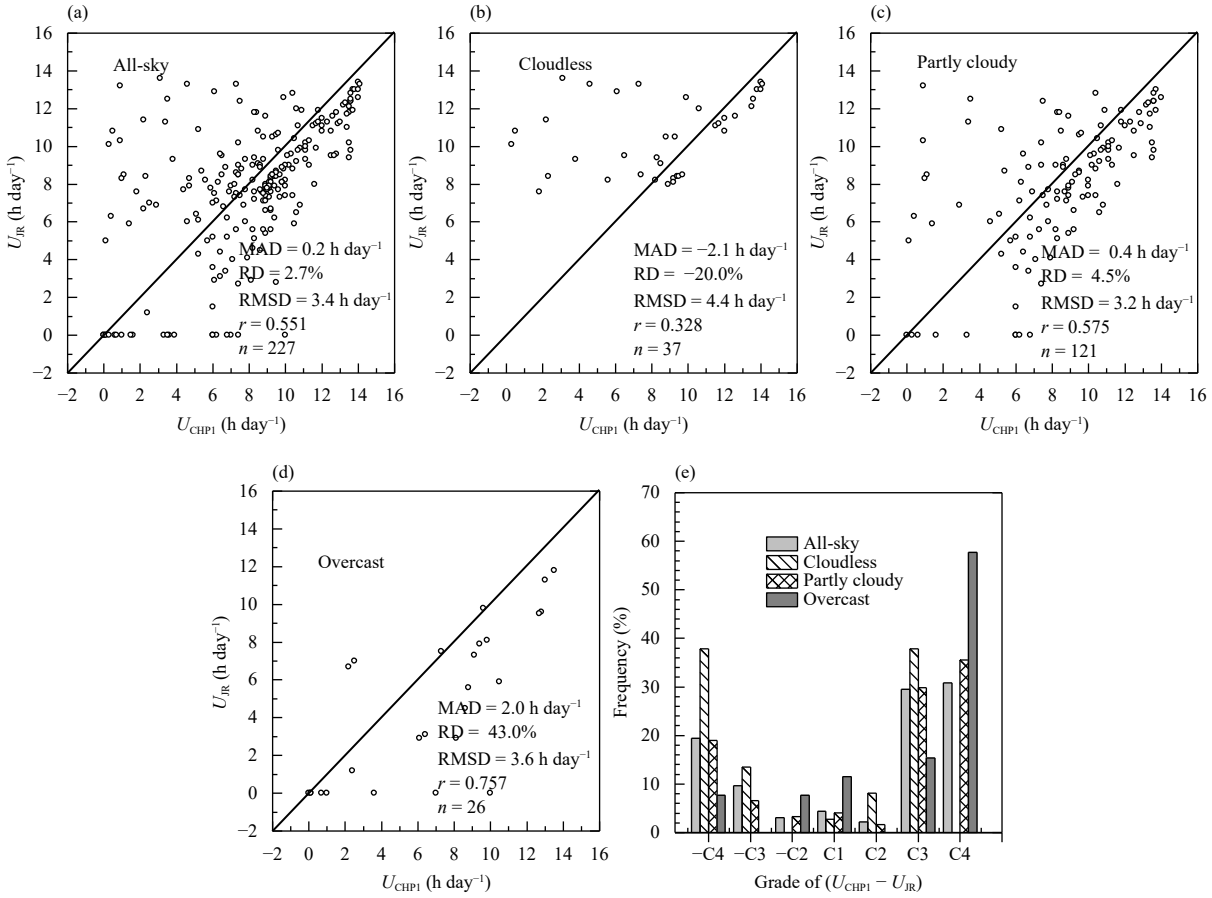


**Fig. 3.** As in Fig. 2, but for the CHP1 pyrheliometer.

**Table 2.** Partial and multiple correlation coefficients between differences in sunshine duration and the influencing factors

| | Partial correlation coefficient ($r_p$) | | | | | Multiple correlation coefficient ($r_m$) | $n$ |
|---|---|---|---|---|---|---|---|
| | $\mu$ | $t$ | $f$ | $S_m$ | $v$ | | |
| $\Delta U_{DFC2_JR}$ | −0.254 | 0.104* | −0.130 | −0.048 | 0.068* | 0.289* | 2801 |
| $\Delta U_{CHP1_JR}$ | −0.270 | 0.098* | −0.001 | −0.096 | 0.021 | 0.301 | 2607 |
| $\Delta U_{CMP11_JR}$ | −0.269 | 0.118* | −0.143 | −0.054 | 0.077* | 0.309* | 2799 |

*Passed the significance test at $\alpha = 0.05$.

stable (~0.5 h h$^{-1}$) because the accuracy of solar tracking was limited when the solar zenith angle was large (~76°; Fig. 5c). Figure 5d shows that the relative humidity of the atmosphere was very high during this time period and ranged from 69% to 53%. As a result of the influence of humidity on the recording paper in the Jordan sunshine recorder and the inaccuracy of solar tracking by the CHP1 pyrheliometer, $\Delta U_{CHP1_JR}$ showed a positive deviation, whereas $\Delta U_{DFC2_JR}$ and $\Delta U_{CMP11_JR}$ showed negative deviations during this time period (Fig. 5b).

The second time period was 0800–1600 BT, when the hourly values of sunshine duration obtained from the Jordan sunshine recorder and three automatic sensors were very close to each other (Fig. 5a). The variables $\theta_z$ and $f$ showed a clear diurnal variation: $\theta_z$ decreased from 76° at 0800 BT to 42° at noon, and then increased to 62° at 1400 BT, while $f$ decreased from 53% to 27% over the whole time period.

The largest differences occurred in the third time period (1600–2000 BT), in which $\theta_z$ increased from 62° to 87° and $f$ ranged from 27% to 45%. The high humidity weakened the sensitivity of the recording paper in the Jordan sunshine recorder and the large solar zenith angle restricted the access of light into the chamber of the Jordan sunshine recorder. The sunshine duration measurements from the Jordan sunshine recorder were therefore considerably less than those obtained from three automatic sensors. During this time period, $\Delta U_{DFC2_JR}$ and $\Delta U_{CMP11_JR}$ were about 0.16 h h$^{-1}$ and $\Delta U_{CHP1_JR}$ was about 0.3 h h$^{-1}$.

The differences in the hourly sunshine duration between the Jordan sunshine recorder and three automatic

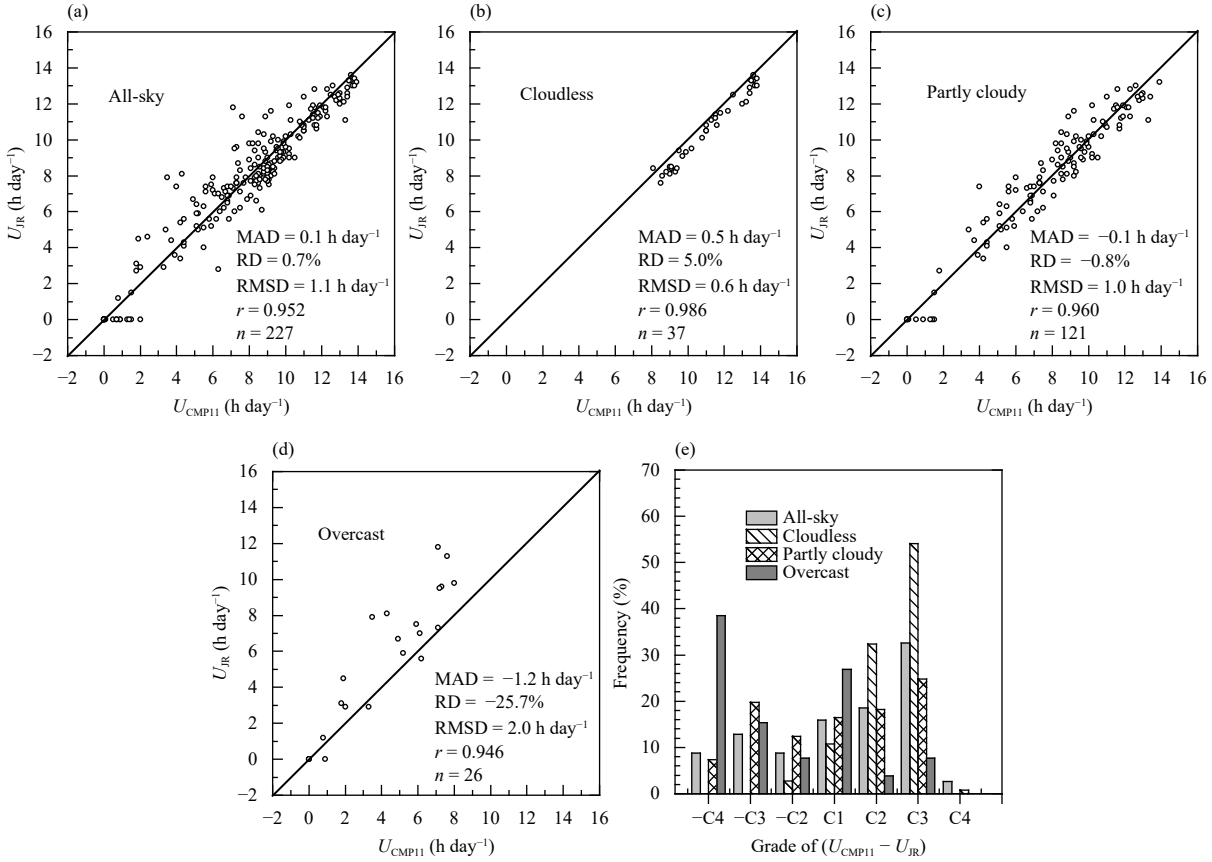


**Fig. 4.** As in Fig. 2, but for the CMP11 pyranometers.

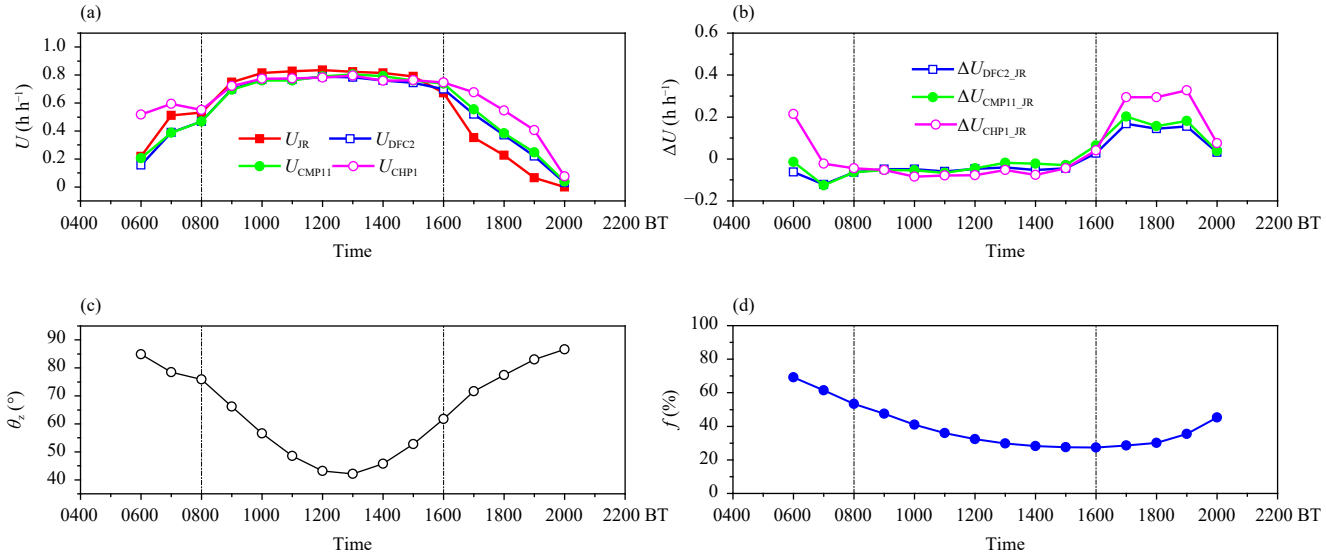


**Fig. 5.** (a) Diurnal variations of hourly sunshine duration obtained from the Jordan sunshine recorder, the DFC2 meter, the CHP1 pyrheliometer, and the CMP11 pyranometers. (b) Differences in measurements by the Jordan sunshine recorder and the DFC2, CHP1, and CMP11 sensors of sunshine duration, (c) the solar zenith angle ($\theta_z$), and (d) the relative humidity ($f$). The dashed lines separate the day into three time periods based on the diurnal variation of sunshine duration.

sensors were primarily caused by the different principles of the sensors and the manufacturing techniques. For example, the method adopted by the CHP1 pyrheliometer is a so-called tracking method, which is affected by the accuracy of the solar tracker. The DFC2 meters uses a static method and remains still during the whole observa-

tional period. The method for sunshine duration measurements used by the CMP11 pyranometers is a semi-static method, in which the global solar irradiance and diffuse irradiance are observed by the CMP11 pyranometers with and without shading, respectively. The shading ball moves with the solar tracker, but the two pyranometers are static. The Jordan sunshine recorder was one of the earliest static instruments. Previous studies have shown that the Jordan sunshine recorder underestimates the sunshine duration two to three hours after sunrise or before sunset when the solar rays cannot pass through the small apertures. By contrast, the large aperture angle (5°) of the CHP1 pyrheliometer means that the circumsolar radiation from a small annular area around the solar disk produces additional radiation and increases the sunshine duration measurement.

The spectral range of the CHP1 pyrheliometer (280–4000 nm) is wider than that of the CMP11 pyranometers (305–2800 nm) and the DFC2 (400–1100 nm) sensor. Based on the solar spectral irradiance dataset recommend by the WMO (Iqbal, 1983), the direct normal solar irradiance at the top of the atmosphere in the spectral ranges of the CHP1 pyrheliometer, the CMP11 pyranometers, and the DFC2 meter was calculated as 1347.6, 1315.7, and 906.5 W $m^{-2}$, respectively. Therefore, if the threshold value of 120 W $m^{-2}$ is adopted to determine the sunshine duration in terms of the measured direct normal solar irradiance, $U_{CHP1}$ will be greater than $U_{CMP11}$ and $U_{DFC2}$.

The detectors used by the automatic sensors also need to be taken into account. The DFC2 uses a photodiode that has a triangular-shaped spectral response function in the spectral range of 400–1100 nm, whereas the CHP1 pyrheliometer and CMP11 pyranometers use thermopiles, which have a fairly straight spectral response function over wider spectral ranges (Wood et al., 2003).

The Jordan sunshine recorder underestimated the hourly sunshine duration in the first and third periods relative to three automatic sensors, but overestimated it in the second period. This means that the daily sunshine duration obtained from the Jordan sunshine recorder may be close to the values obtained from the DFC2 meter and the CMP11 pyranometers as a result of compensation effects in the diurnal variation of the hourly sunshine duration.

## 4. DFC2-equivalent sunshine duration estimation (DFCESD) model

### 4.1 *Construction of the DFCESD model*

Our comparisons with the other instruments show that the DFC2 meter is suitable for measuring sunshine duration. Based on its high degree of automation, simplicity, reliability, and low cost, the DFC2 meter is recommended by the CMA as an alternative to the Jordan sunshine recorder in observations of sunshine duration by meteorological stations in China. However, the long-term records of sunshine duration at most of these meteorological stations were made by using the Jordan sunshine recorder. It is therefore necessary to establish a regression function to improve the homogeneity of long-term sunshine duration data in climate studies in this region. We refer to this function as the DFCESD model. This model can be used to adjust the sunshine duration measurements from the Jordan sunshine recorder to the same level as those measured by the DFC2 meter. Fortunately, there is a high linear correlation between the daily sunshine duration from the Jordan sunshine recorder and that from the DFC2 meter.

We used a dataset of 184 daily sunshine duration data pairs from parallel observations by the two instruments in the time period 1 January–4 July 2019 and the least squares method to derive a simple linear regression model:

$$U_{DFC2_JR} = -0.0723 + 1.0882 \times U_{JR}, \quad (8)$$

where $U_{DFC2_JR}$ is the DFC2-equivalent daily sunshine duration. The determination coefficient of Eq. (8) is 0.945, which indicates a high goodness of fit.

### 4.2 *Verification of the DFCESD model*

We used another dataset consisting of 117 daily sunshine duration measurements obtained from the Jordan sunshine recorder and the DFC2 meter over the time period 3 November 2020–28 February 2021 with the DFCESD model to generate the daily DFC2-equivalent sunshine duration and to evaluate the accuracy of the model. The daily sunshine duration measurements from the DFC2 meter are plotted against both the daily sunshine duration observed from the Jordan sunshine recorder (Fig. 6a) and the sunshine duration estimated by the DFCESD model using daily measurements from the Jordan sunshine recorder (Fig. 6b). Histograms of the differences between the daily sunshine duration obtained from the Jordan sunshine recorder and the DFC2 meter ($U_{JR} - U_{DFC2}$) and those between the estimated DFC2 and those observed by the DFC2 meter ($U_{DFC2_JR} - U_{DFC2}$) are plotted against the grades of Urban and Zając (2017) (Figs. 6c, d).

Figures 6a and 6b show that the MAD between $U_{JR}$ and $U_{DFC2}$ increased from −0.7 to −0.2 h $day^{-1}$ after correction by the DFCESD model, the RD increased from

−9.3% to −2.3%, and the RMSD decreased from 1.0 to 0.8 h day$^{-1}$. The histograms of differences in daily sunshine duration were more evenly distributed in all grades. The results of the verification showed that the DFCESD model improves the consistency of the daily sunshine duration measurements between $U_{DFC2}$ and $U_{JR}$ and can be used in further studies, such as the construction of a long-term homogeneous sunshine duration dataset based on daily sunshine duration data measured by both the Jordan sunshine recorder and the DFC2 meter.

## 5. Conclusions and discussion

We analyzed sunshine duration measurements obtained from the Jordan sunshine recorder and three automatic sensors located at the SDZ over the time periods 1 January–5 July 2019 and 3 November 2020–28 February 2021. Our conclusions are as follows.

(1) The differences in daily sunshine duration obtained from the Jordan sunshine recorder and the DFC2 meter, the CHP1 pyrheliometer, and the CMP11 pyranometers varied with the sky conditions. The sunshine duration observed by the Jordan sunshine recorder on clear days was generally less than that observed by the DFC2 photoelectric sensor and the CHP1 and CMP11 thermoelectric radiation meters. With an increase in cloud cover and the appearance of low- or medium-level clouds (cumulus, cumulonimbus, and altocumulus clouds), the Jordan sunshine recorder occasionally overestimated the sunshine duration because the cumulus clouds moved so quickly that short, high-intensity bursts of sunlight cre-

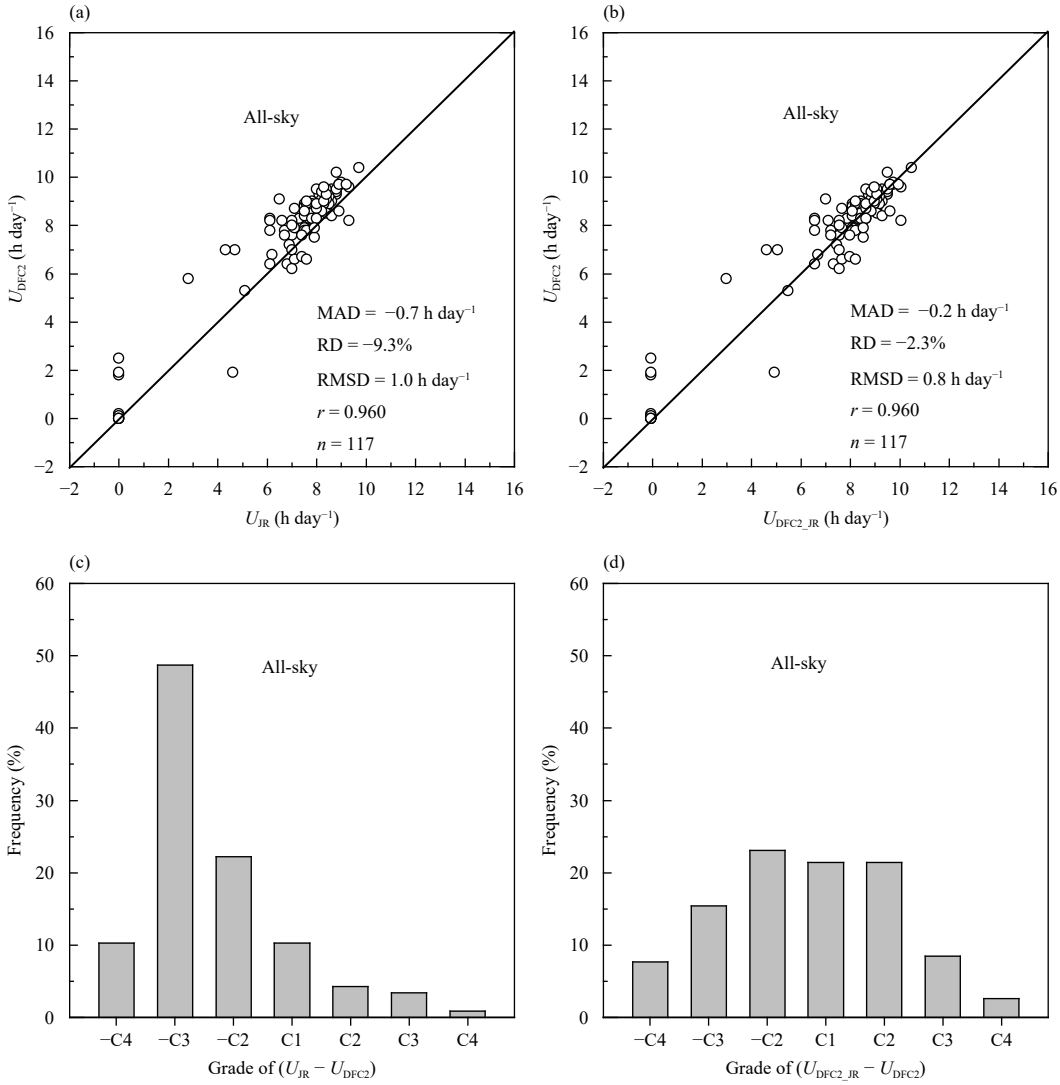


**Fig. 6.** Scatterplots of daily sunshine duration measurements from the DFC2 meter ($U_{DFC2}$) versus (a) those from the Jordan sunshine recorder ($U_{JR}$) and (b) from the Jordan sunshine recorder corrected by the DFCESD model ($U_{DFC2_JR}$). Histograms of (c) $U_{JR} - U_{DFC2}$ and (d) $U_{DFC2_JR} - U_{DFC2}$ plotted against the classification grades of Urban and Zając (2017).

ated an overlapping tracing effect on the recording cards.

(2) The patterns in the diurnal variation of the hourly sunshine duration obtained from the Jordan sunshine recorder and three automatic sensors were different as a result of their different principles and structures. For instance, the hourly sunshine duration observed by the Jordan sunshine recorder was less than that observed by the automatic sensors two to three hours after sunrise or before sunset. This is when fewer solar rays are able to enter the Jordan sunshine recorder through the small apertures. By contrast, the automatic sensors were usually exposed to the sunshine throughout the day, which resulted in larger values for sunshine duration than the Jordan sunshine recorder.

(3) The DFC2 meter uses a photodiode as its detector, whereas the CHP1 pyrheliometer and the CMP11 pyranometers use thermopiles. The fundamental principle of measurements of solar radiation by the photodiode is based on the photovoltaic effect—that is, the solar irradiance reaching the photodiode is first converted into an electric current and then to a voltage with the aid of a resistor. The thermopile uses several pairs of thermocouple junctions to measure solar radiation. The spectral ranges of the photodiode and thermopile are different: the spectral range of the photodiode sensor of the DFC2 is between 400 and 1100 nm, whereas the spectral ranges for the CHP1 pyrheliometer and the CMP11 pyranometers are 280–4000 and 305–2800 nm, respectively. The spectral response function of the DFC2 meter is a triangular shaped line with a peak at certain wavelengths, whereas the spectral response functions of the CHP1 pyrheliometer and the CMP11 pyranometers are relatively smooth over wide spectral ranges.

(4) The solar zenith angle, relative humidity, and air temperature are the most important factors influencing the differences in sunshine duration between the Jordan sunshine recorder and three automatic sensors.

(5) We established a DFCESD model through which the daily sunshine duration measurements from the Jordan sunshine recorder could be adjusted to the same level as those measured by the DFC2 meter.

In summary, the daily sunshine duration obtained from the Jordan sunshine recorder is consistent with the measurements obtained by the DFC2 meter and the CMP11 pyranometers. A long-term consistent daily sunshine duration dataset was established by using the sunshine duration observations from the Jordan sunshine recorder and the DFC2 meter in conjunction with a regression model. The fast response, small volume, and low cost of the DFC2 meter mean that it can be used as an alternative to the Jordan sunshine recorder in operational observations of sunshine duration.

***Acknowledgments.*** We thank the anonymous reviewers and editors for their valuable and stimulating comments, which have greatly improved our paper. We also thank Dawei Li from Huayun Sounding (Beijing) Co. Ltd. for providing the user guide for the DFC2 photoelectric sunshine meter and some constructive suggestions.

## REFERENCES

Babikir, M. H., D. Njomo, M. Y. Khayal, et al., 2018: Estimation of direct solar radiation of Chad. *Energ. Power Eng.*, **10**, 212–225, doi: 10.4236/epe.2018.105015.

Baumgartner, D. J., W. Pötzi, H. Freislich, et al., 2018: A comparison of long-term parallel measurements of sunshine duration obtained with a Campbell-Stokes sunshine recorder and two automated sunshine sensors. *Theor. Appl. Climatol.*, **133**, 263–275, doi: 10.1007/s00704-017-2159-9.

Brázdil, R., A. A. Flocas, and H. S. Sahsamanoglou, 1994: Fluctuation of sunshine duration in central and south-eastern Europe. *Int. J. Climatol.*, **14**, 1017–1034, doi: 10.1002/joc.3370140907.

Gueymard, C., 1993: Analysis of monthly average solar radiation and bright sunshine for different thresholds at Cape Canaveral, Florida. *Sol. Energy*, **51**, 139–145, doi: 10.1016/0038-092X(93)90075-Y.

Helmes, L., and R. Jaenicke, 1984: Experimental verification of the determination of atmospheric turbidity from sunshine recorders. *J. Climate Appl. Meteor.*, **23**, 1350–1353, doi: 10.1175/1520-0450(1984)023<1350:EVOTDO>2.0.CO;2.

Hinssen, Y. B. L., and W. H. Knap, 2007: Comparison of pyranometric and pyrheliometric methods for the determination of sunshine duration. *J. Atmos. Oceanic Technol.*, **24**, 835–846, doi: 10.1175/JTECH2013.1.

Horseman, A., A. R. MacKenzie, and R. Timmis, 2008: Using bright sunshine at low-elevation angles to compile an historical record of the effect of aerosol on incoming solar radiation. *Atmos. Environ.*, **42**, 7600–7610, doi: 10.1016/j.atmosenv.2008.06.033.

Hoyt, D. V., 1977: Percent of possible sunshine and the total cloud cover. *Mon. Wea. Rev.*, **105**, 648–652, doi: 10.1175/1520-0493(1977)105<0648:POPSAT>2.0.CO;2.

Huayun Sounding, 2018: User Manual of DFC2 Photoelectric Sunshine Meter. Huayun Sounding (Beijing) Meteorological Technology Co. Ltd., Beijing, 1–20.

Iqbal, M., 1983: *An Introduction to Solar Radiation*. Academic Press, Ontario, Canada, 390 pp.

Jaenicke, R., and F. Kasten, 1978: Estimation of atmospheric turbidity from the burned traces of the Campbell-Stokes sunshine recorder. *Appl. Opt.*, **17**, 2617–2621, doi: 10.1364/AO.17.002617.

Jordan, J. B., 1888: Jordan's new pattern photographic sunshine recorder. *Quart. J. Roy. Meteor. Soc.*, **14**, 212–217, doi: 10.1002/qj.4970146704.

Kerr, A., and R. Tabony, 2004: Comparison of sunshine recorded by Campbell–Stokes and automatic sensors. *Weather*, **59**, 90–95, doi: 10.1256/wea.99.03.

Kipp & Zonen, 2008: CHP1 Pyrheliometer Instruction Manual. Version 0811, Kipp & Zonen, Delft, Netherlands, 23 pp.

Kipp & Zonen, 2016: Instruction Manual for CMP Series Pyranometer and CMA Series Albedometer. No. V1610, Kipp & Zonen, Delft, Netherlands, 1–45.

Legg, T., 2014: Comparison of daily sunshine duration recorded by Campbell–Stokes and Kipp and Zonen sensors. *Weather*, **69**, 264–267, doi: 10.1002/wea.2288.

Li, J. R., D. J. Qian, and H. M. Zhu, 1989: Threshold analysis of Jordan sunshine recorder. *J. Chengdu Meteor. Inst.*, 58–63. (in Chinese)

Lin, W., X. Xu, X. Zhang, et al., 2008: Contributions of pollutants from North China Plain to surface ozone at the Shangdianzi GAW Station. *Atmos. Chem. Phys.*, **8**, 5889–5898, doi: 10.5194/acp-8-5889-2008.

Long, C. N., and Y. Shi, 2008: An automated quality assessment and control algorithm for surface radiation measurements. *Open Atmos. Sci. J.*, **2**, 23–37, doi: 10.2174/1874282300802010023.

Matuszko, D., 2012: Influence of cloudiness on sunshine duration. *Int. J. Climatol.*, **32**, 1527–1536, doi: 10.1002/joc.2370.

Matuszko, D., 2015: A comparison of sunshine duration records from the Campbell-Stokes sunshine recorder and CSD3 sunshine duration sensor. *Theor. Appl. Climatol.*, **119**, 401–406, doi: 10.1007/s00704-014-1125-z.

Ohmura, A., E. G. Dutton, B. Forgan, et al., 1998: Baseline Surface Radiation Network (BSRN/WCRP): New precision radiometry for climate research. *Bull. Amer. Meteor. Soc.*, **79**, 2115–2136, doi: 10.1175/1520-0477(1998)079<2115:BSRNBW>2.0.CO;2.

Painter, H. E., 1981: The performance of a Campbell–Stokes sunshine recorder compared with a simultaneous record of the normal incidence irradiance. *Meteor. Mag.*, **110**, 102–109.

Pandey, P. K., P. P. Dabral, and V. Pandey, 2016: Evaluation of reference evapotranspiration methods for the northeastern region of India. *Int. Soil Water Conserv. Res.*, **4**, 52–63, doi: 10.1016/j.iswcr.2016.02.003.

Raju, A. S. N., and K. K. Kumar, 1982: Comparison of point cloudiness and sunshine derived cloud cover in India. *Pure Appl. Geophys.*, **120**, 495–502, doi: 10.1007/bf00879832.

Ranzi, R., and R. Rosso, 1995: Distributed estimation of incoming direct solar radiation over a drainage basin. *J. Hydrol.*, **166**, 461–478, doi: 10.1016/0022-1694(94)05099-J.

Sanchez-Lorenzo, A., J. Calbó, M. Wild, et al., 2013: New insights into the history of the Campbell-Stokes sunshine recorder. *Weather*, **68**, 327–331, doi: 10.1002/wea.2130.

Sanchez-Romero, A., A. Sanchez-Lorenzo, J. Calbó, et al., 2014: The signal of aerosol-induced changes in sunshine duration records: A review of the evidence. *J. Geophys. Res. Atmos.*, **119**, 4657–4673, doi: 10.1002/2013JD021393.

Sanchez-Romero, A., J. A. González, J. Calbó, et al., 2015: Using digital image processing to characterize the Campbell–Stokes sunshine recorder and to derive high-temporal resolution direct solar irradiance. *Atmos. Meas. Tech.*, **8**, 183–194, doi: 10.5194/amt-8-183-2015.

Stanhill, G., 2003: Through a glass brightly: Some new light on the Campbell–Stokes sunshine recorder. *Weather*, **58**, 3–11, doi: 10.1256/wea.278.01.

Urban, G., and I. Zając, 2017: Comparison of sunshine duration measurements from Campbell-Stokes sunshine recorder and CSD1 sensor. *Theor. Appl. Climatol.*, **129**, 77–87, doi: 10.1007/s00704-016-1762-5.

Wang, H. S., D. S. Liu, H. Lin, et al., 2015: NDVI and vegetation phenology dynamics under the influence of sunshine duration on the Tibetan plateau. *Int. J. Climatol.*, **35**, 687–698, doi: 10.1002/joc.4013.

WMO, 1982: Commission for Instruments and Methods of Observation—Abridged Final Report of the Eighth Session. WMO-No. 590, WMO, Mexico City, 111 pp.

WMO, 2006: Guide to Meteorological Instruments and Methods of Observation. WMO-No. 8, WMO, Geneva, 569 pp.

Wood, J., T. Muneer, and J. Kubie, 2003: Evaluation of a new photodiode sensor for measuring global and diffuse irradiance, and sunshine duration. *J. Sol. Energ. Eng.*, **125**, 43–48, doi: 10.1115/1.1531149.

Yang, H. H., L. Y. Wang, and X. H. Wang, 2017: Research on improving the measurement accuracy of photoelectric sunshine meter. *J. Changchun Univ. Sci. Tech. (Nat. Sci. Ed.)*, **40**, 25–28, 35, doi: 10.3969/j.issn.1672-9870.2017.05.007. (in Chinese)

Zhang, W. M., and Y. X. Tan, 2000: Approach error of sunshine recorder. *Meteor. Mon.*, **26**, 17–19, doi: 10.3969/j.issn.1000-0526.2000.05.004. (in Chinese)

Zhu, X. C., X. F. Qiu, Y. Zeng, et al., 2015: A remote sensing model to estimate sunshine duration in the Ningxia Hui Autonomous Region, China. *J. Meteor. Res.*, **29**, 144–154, doi: 10.1007/s13351-015-4059-1.

Tech & Copy Editor: Qi WANG